Biochimica et Biophysica Acta 1827 (2013) 1383–1391

Contents lists available at ScienceDirect

Biochimica et Biophysica Acta

journal homepage: www.elsevier.com/locate/bbabio

Alternative Complex III from phototrophic bacteria and its electron acceptor auracyanin ☆

Erica L.W. Majumder, Jeremy D. King, Robert E. Blankenship *

Washington University in St. Louis, Departments of Biology and Chemistry, Campus Box 1137, One Brookings Dr, St. Louis, MO 63130, USA

ARTICLE INFO

Article history:
Received 20 July 2012
Received in revised form 12 January 2013
Accepted 15 January 2013
Available online 25 January 2013

Keywords:
Alternative Complex III
Auracyanin
Blue copper proteins
Cytochrome bc_1 complex
Cytochrome b_6f complex

ABSTRACT

Alternative Complex III (ACIII) is a multisubunit integral membrane protein electron transfer complex that is proposed to be an energy-conserving functional replacement for the bacterial cytochrome bc_1 or b_6f complexes. Clues to the structure and function of this novel complex come from its relation to other bacterial enzyme families. The ACIII complex has menaquinone: electron acceptor oxidoreductase activity and contains protein subunits with multiple Fe–S centers and *c*-type hemes. ACIII is found in a diverse group of bacteria, including both phototrophic and nonphototrophic taxa. In the phototrophic filamentous anoxygenic phototrophs, the electron acceptor is the small blue copper protein auracyanin instead of a soluble cytochrome. Recent work on ACIII and the copper protein auracyanin is reviewed with focus on the photosynthetic systems and potential electron transfer pathways and mechanisms. Taken together, the ACIII complexes constitute a unique system for photosynthetic electron transfer and energy conservation. This article is part of a Special Issue entitled: Respiratory Complex III and related *bc* complexes.

1. Introduction

In order to survive, organisms need mechanisms to convert and store energy. For all organisms, this involves the establishment of a proton motive force (PMF) or a cross membrane charge gradient by coupling thermodynamically favorable electron transport to proton pumping or ion translocation. For anoxygenic phototrophs, this involves cyclic electron flow around a reaction center and a proton pump. In such systems, the reaction center uses light energy to reduce a quinone to a quinol. The quinol is subsequently oxidized by the proton pump to establish the PMF, and the electrons are donated back to the reaction center via a periplasmic electron carrier [1]. Until very recently, it was thought that the cytochrome bc_1 or the related cytochrome b_6f complex were the only complexes able to oxidize quinol and reduce a periplasmic electron carrier in phototrophic organisms. A putative functional replacement for the cytochrome bc_1 complex has been characterized in the filamentous anoxygenic phototroph *Chloroflexus aurantiacus*. The complex has been named Alternative Complex III. The complex itself is structurally and evolutionarily unrelated to the cytochrome bc_1 or cytochrome b_6f complexes. Instead, it is a new member of the complex iron–sulfur molybdoenzyme (CISM) superfamily.

The filamentous anoxygenic phototrophs (FAPs) are photosynthetic members of the Chloroflexi phylum. The founding member of this phylum, *C. aurantiacus*, was characterized in 1974 by Beverly Pierson and Richard Castenholz [2]. It was originally described as a thermophilic photoheterotroph similar in terms of photosynthetic metabolism to purple phototrophic bacteria. Subsequently, it has been shown to be capable of photoautotrophic growth using the hydroxypropionate cycle instead of the Calvin–Benson cycle [3]. The discovery of its type II reaction center prompted further comparisons with purple phototrophic bacteria [4]. Despite the presence of very similar reaction center and integral membrane light-harvesting complexes to those found in the purple bacteria, biochemical and spectroscopic techniques failed to identify a cytochrome bc_1 complex [5]. In the 1980s, a novel group of blue copper proteins were identified in *C. aurantiacus* [6]. The proteins were named auracyanins. Their similar nature to plastocyanin from oxygenic phototrophs and their ability to re-reduce the *C. aurantiacus* reaction center led to the conclusion that the auracyanins functioned as periplasmic electron carriers [7]. A more in-depth characterization of the heme-containing complexes in *C. aurantiacus* led to the discovery of ACIII [8]. Enzyme activity assays subsequently demonstrated ACIII's capacity to oxidize quinol and reduce auracyanins [9].

2. Discovery of ACIII

Evidence for ACIII came from two separate sources, a respiratory complex in the nonphototrophic thermophilic bacterium *Rhodothermus marinus* and a photosynthetic complex in *C. aurantiacus* [10,11]. Initially, the proteins were thought to be unrelated, but were later identified as related complexes. In both cases, the membranes of the bacteria

☆ This article is part of a Special Issue entitled: Respiratory Complex III and related *bc* complexes.

* Corresponding author. Tel.: +1 314 935 7971.
E-mail address: Blankenship@wustl.edu (R.E. Blankenship).

0005-2728/$ – see front matter © 2013 Elsevier B.V. All rights reserved.
http://dx.doi.org/10.1016/j.bbabio.2013.01.008

were investigated for electron transfer chain components, but no typical Complex III, cytochrome bc_1 complex, was detected [12,13]. The activity usually held by Complex III, menaquinone: electron acceptor oxidoreductase, was observed despite the lack of the traditional complex leading to the search for ACIII [9]. In *R. marinus*, the isolated complex was originally thought to contain *b* and *c* type hemes and donate to a soluble high-potential iron protein (HiPIP) [14]. Work in the *C. aurantiacus* system yielded a complex with only *c* type hemes and was recognized to have high homology with the CISM family [8]. The complex was originally named MFIcc, but after no molybdenum was found the name was changed to ACIII [15]. In *C. aurantiacus* a distinct respiratory ACIII was found under chemotrophic growth. The respiratory and photosynthetic complexes from both *C. aurantiacus* and *R. marinus* were then identified as ACIII when the electron transport activity was confirmed and the genomes sequenced [9,16]. ACIII is widely distributed in a variety of bacterial phyla and represents a novel mechanism and structure for Complex III or cytochrome bc_1 activity since the ACIII is structurally and evolutionarily unrelated to either complex [17].

3. Protein subunits of ACIII

ACIII is a novel integral membrane protein complex with five to seven subunits coded for by genes on one putative operon. Several subunits of ACIII contain high homology to subunits of the energy converting complex iron–sulfur molybdoenzyme, CISM, protein family. Relations to this family provide clues to understand ACIII. ACIII is composed of 22 putative transmembrane helices, iron–sulfur clusters, *c*-type hemes and a putative quinol oxidation site. The subunits of ACIII have been named ActA through ActG, with the genes that code for them named *actA* through *actG*. ActG is not found in all organisms that contain the ACIII complex, and in some cases the gene order is different than in *C. aurantiacus* (Fig. 1). Typically in ACIII ActA is a pentaheme subunit with one transmembrane helix and ActB contains iron–sulfur clusters. Act C & F are responsible for most of the transmembrane helices and the probable quinone binding regions while ActD contributes one transmembrane helix. ActE is a monoheme periplasmic subunit and ActG is a periplasmic subunit of unknown function. In the *C. aurantiacus* respiratory complex, the gene cluster only has *actBEAG* in that order and is missing *actCDF* (Fig. 1). However, the full complex has all seven subunits, presumably resulting from transcription of some of the genes in the phototrophic gene cluster. The gene cluster comprising the subunits of ACIII forms a putative operon, although this has not been demonstrated experimentally.

3.1. ActA

ActA is a 25 kDa pentaheme protein that is predicted to be oriented in the periplasm with an N-terminal transmembrane helix anchoring the subunit [15,18]. Biochemical prediction software labels the N-terminal region as both a transmembrane helix and a signal peptide [19,20]. For *C. aurantiacus*, mass spectrometry data has shown that the N-terminal region is not cleaved in the native protein, indicating the presence of a transmembrane helix not a signal peptide (data not shown). This putative transmembrane helix is predicted to serve as a membrane anchor (Fig. 1). Yet, in the related *Escherichia coli* nitrite reductase second pentaheme subunit, NrfB, the N-terminal region is a signal peptide that is cleaved off after translocation to the periplasm [21]. Basic homology modeling of this subunit has been performed using the pentaheme subunit from *E. coli* nitrite reductase, NrfB, as a template (Fig. 2A) [22–25]. The overall alignment, with the N-terminal signal peptide region truncated, is useful for modeling with 40% similarity, and presents a first look at a potential structure for ActA. NrfB contains hemes with both parallel and perpendicular orientations; however, the sequence in ActA does not contain the residues that typically indicate a parallel heme motif [21]. Therefore ActA may only have perpendicular hemes, so the orientation of the hemes in the model is not certain. The full protein has also been modeled with the N-terminal and C-terminal ends of

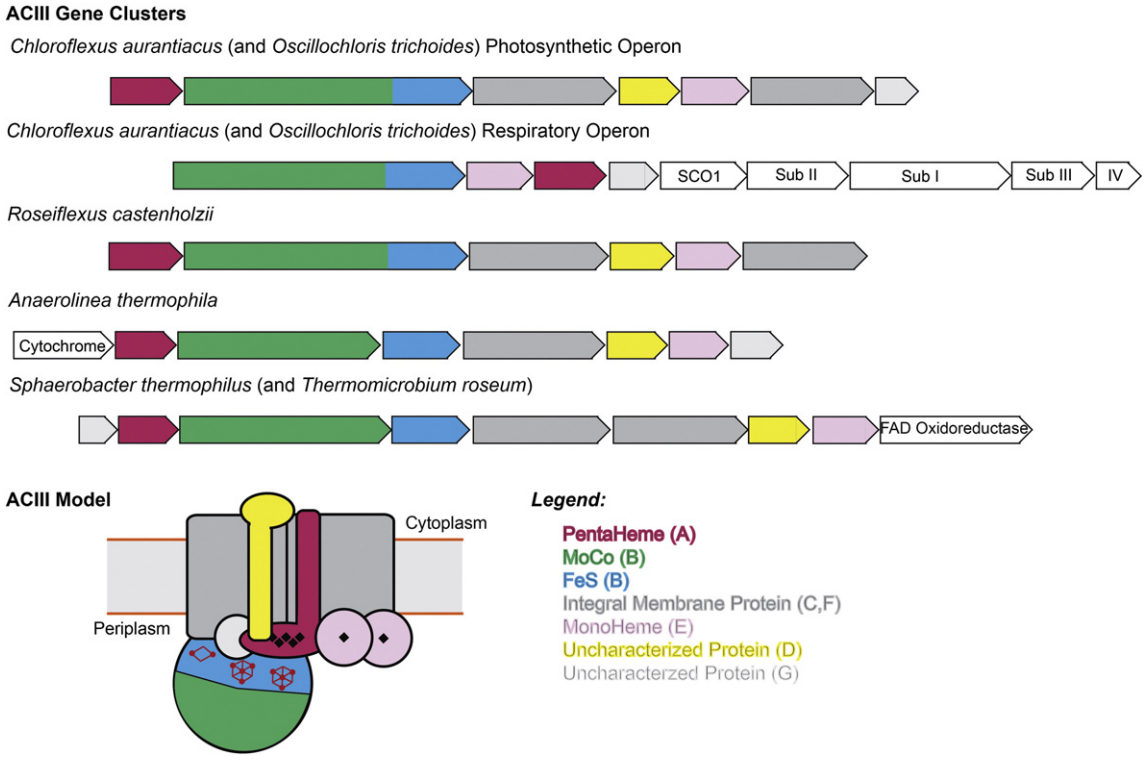

Fig. 1. Current model of ACIII. ACIII photosynthetic and respiratory operons from several bacteria. Schematic structure of ACIII as predicted by cross-linking data and topology and homology prediction.

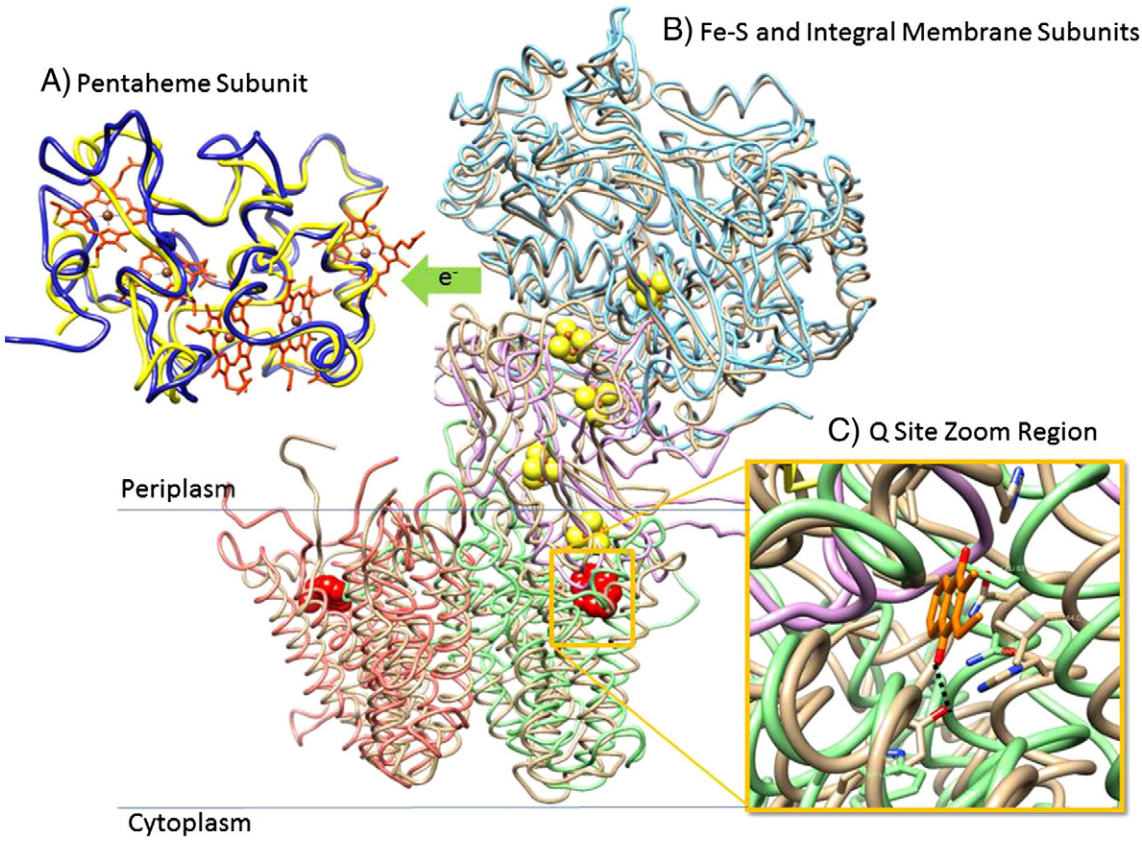

Fig. 2. Homology model of selected subunits of ACIII. A. ActA (blue) modeled onto NrfB, Protein Data Bank file 2OZY (yellow). C type hemes (brown dot with orange-red ligands) are from NrfB. Green arrow denotes putative flow of electrons. B. ActB1 (blue), ActB2 (purple), ActC (green) and ActF (pink) independently modeled onto corresponding PDB entry, 2VPW, PsrABCG subunits (tan). Iron–sulfur clusters (yellow), menaquinone-7 (red) and the molybdopterin cofactor (magenta) are from PSR. C. Zoom in of the quinone binding site with MK-7(orange) bound. Subunits making up the pocket are ActC (green), ActB2 (purple) and PsrBC (tan). Side chains of potential hydrogen bonding or other important residues are shown. The known H-bond from PSR is shown (black dashed line).

the dodecaheme protein, cytochrome *c* GSU1996, from *Geobacter sulfurreducens* (data not shown), revealing that ActA has similarity to other multiheme proteins involved in electron transport [26]. Despite having an additional heme and not being related to ACIII, the *Geobacter* protein has higher similarity and identity (Supplemental Table 1). The homology model in Fig. 2 is an approximation of the structure of four subunits of this complicated enzyme.

Multiheme proteins are involved in electron transport, where the hemes form a nanowire for efficient electron transfer [26]. The heme redox potentials in ActA for *C. aurantiacus* were determined as −228 mV, −110 mV and +94 mV with a ratio of 3:1:1 respectively. The two remaining redox potentials were +391 mV and belong to a dimeric monoheme subunit, ActE [15]. Redox titration measurement of the whole complex in *R. marinus* showed a redox potential range of −45 to +235 mV [12]. There is a large difference in the measurement of the redox potentials for the complexes, which may result from having different electron acceptors or being part of different cycles. ActA has not been shown to house another cofactor or active site, so the subunit should be performing electron transfer and not additional chemistry. Following heme reduction potentials, ActA should donate its electrons to another subunit, most probably the monoheme subunit, ActE [27]. Many enzymes in nature extend their heme nanowires by donating to an additional adjacent heme subunit, as would be the case in ACIII if ActA donated to ActE. This would also follow the expected increase in redox potential needed for electron transfer. The electron donor to the pentaheme subunit is still unknown. The electrons could come directly from the quinol oxidation site. A second plausible electron source is the Fe–S clusters from ActB, which will be discussed in the next section.

3.2. ActB

ActB is the largest subunit of the ACIII complex with a mass of ca. 113 kDa and is a putative gene fusion product of two smaller genes [8]. The domain referred to as B1 has high homology to subunits that contain a molybdopterin cofactor. Atomic absorption determination of ACIII has not detected molybdenum, manganese, or tungsten [15]. Mo-cofactor binding residues are not conserved in ActB [27]. Similar mutations occur in other complexes with CISM family-like catalytic subunits that also lack molybdenum, such as Respiratory Complex I [28]. Other members of the CISM family have replaced the Mo-cofactor with W, Ni or a lone Fe–S cluster [29]. Thus far, there is no evidence for a cofactor in the B1 domain of ActB from ACIII. B1 comes first in the gene and is putatively located on top of B2 further away from the membrane (Fig. 1). B1 aligns well with many members of the CISM family and homology modeling has been performed with the Mo-co subunit from polysulfide reductase, PSR, from *Thermus thermophilus* (Fig. 2B) [30]. Despite the presumed lack of a pterin-like cofactor and no S_0 iron–sulfur cluster in B1, the model provides a general sense of the structure but does not provide new clues as to the function of the B1 domain. The B1 domain does contain the Twin Arginine Translocase sequence (TAT) sequence that is reported to promote the translocation of the subunit to the periplasm [31]. However, new debate has arisen over the orientation of the B subunit and this issue will be discussed in more detail below.

The B2 domain is the iron–sulfur cluster-containing domain of the ActB subunit. It is the smaller portion of ActB, being the last ca. 251 of 1029 residues in *C. aurantiacus*. Despite high sequence similarity among

ACIII's from different families, 57% identity between *C. aurantiacus* and *R. marinus*, the number and type of predicted iron–sulfur clusters has varied in the literature. Biochemical evidence in *C. aurantiacus* yields 17 iron atoms per complex, with seven belonging to hemes and the remaining ten to iron–sulfur clusters, which were assigned as one [2Fe–2S] and two [4Fe–4S] based on sequence and number of irons detected [15]. In contrast, biochemical and sequence evidence in *R. marinus* ascribes 21 irons per complex with 15 belonging to one [3Fe–4S] and three [4Fe–4S] [16]. EPR work elucidated the [3Fe–4S] cluster in *R. marinus* with a reduction potential of + 140 mV [12]. Examination of the sequences using known Fe–S binding motifs predicts one [3Fe–4S] and two to three [4Fe–4S]. The third [4Fe–4S] cluster has an atypical motif conserved in all ACIIIs. Typical [4Fe–4S] binding motifs have two residues in between the middle cysteines [32]. Other CISM family Fe–S proteins have more than two residues in the middle with 11–12. ACIII's have 26–33. With the extended spacing, the physiological presence of the third [4Fe–4S] cluster is uncertain. B2 has also been modeled with PsrB (Fig. 2B). PsrB has four [4Fe–4S] clusters in a ferredoxin-like fold, but with the same [Fe–S] binding motifs as ACIII, which has up to four iron–sulfur clusters in B2. In the model, the Fe–S binding motifs align well, but the model of ACIII has additional loops from extra amino acids in the sequence [30]. Since the Fe–S binding amino acids are modeled in the same location, the Fe–S clusters from PSR are presented in the model. Most importantly for function considerations, the position of the iron–sulfur clusters creates pathway for electron transfer from the quinone site in ActC. The exact content for the Fe–S clusters of ACIII across species remains to be determined.

The orientation of the ActB subunit with respect to the membrane has been a topic of debate. Cross-linking data from *C. aurantiacus* placed ActB in cytoplasm [15]. However, a TAT sequence is present on the N-terminus of the protein, which suggests translocation to the periplasm [8,27]. Recent sequence investigation proposed that for the TAT translocation to be active, additional motifs later on in the sequence are necessary, but these motifs are not present in ACIII, again suggesting a cytoplasmic orientation [27]. ActB aligns well with known periplasmic PsrAB (Fig. 2B). Also, the quinone site in PsrC is on the periplasmic face of the membrane and capped by PsrB, so the iron–sulfur clusters of PsrB are within electron transfer distance. The quinone site of ActC aligns on the periplasmic face by homology model and topology prediction, again suggesting a periplasmic location for ActB to facilitate electron transfer to the iron–sulfur clusters (Figs. 2B & C & 3A) [33,34]. Likewise, cross-linking data shows that ActB and ActC interact [15]. However, in ACIII, the whole unit of ActBC could be flipped to the cytoplasm, which preserves the needed quinone–Fe–S interactions. Finally, a verification calculation of the predicted topologies was performed using the extrinsic loop similarity method of Weiner [35]. The simple calculation method yielded small agreement with a periplasmic orientation with a value of 0.222 over the loop similarity average for the CISM NrfD family, but the empirical calculation showed moderate agreement with cytoplasmic orientation (Supplemental Fig. 1 and Tables 2 & 3). A similar debate has existed in the case of DMSO reductase from *E. coli* for over twenty years, as biochemical and sequence based evidence continues to accrue [36–38]. DmsABC was the only family presented by Weiner where the calculation did not agree with the experimental

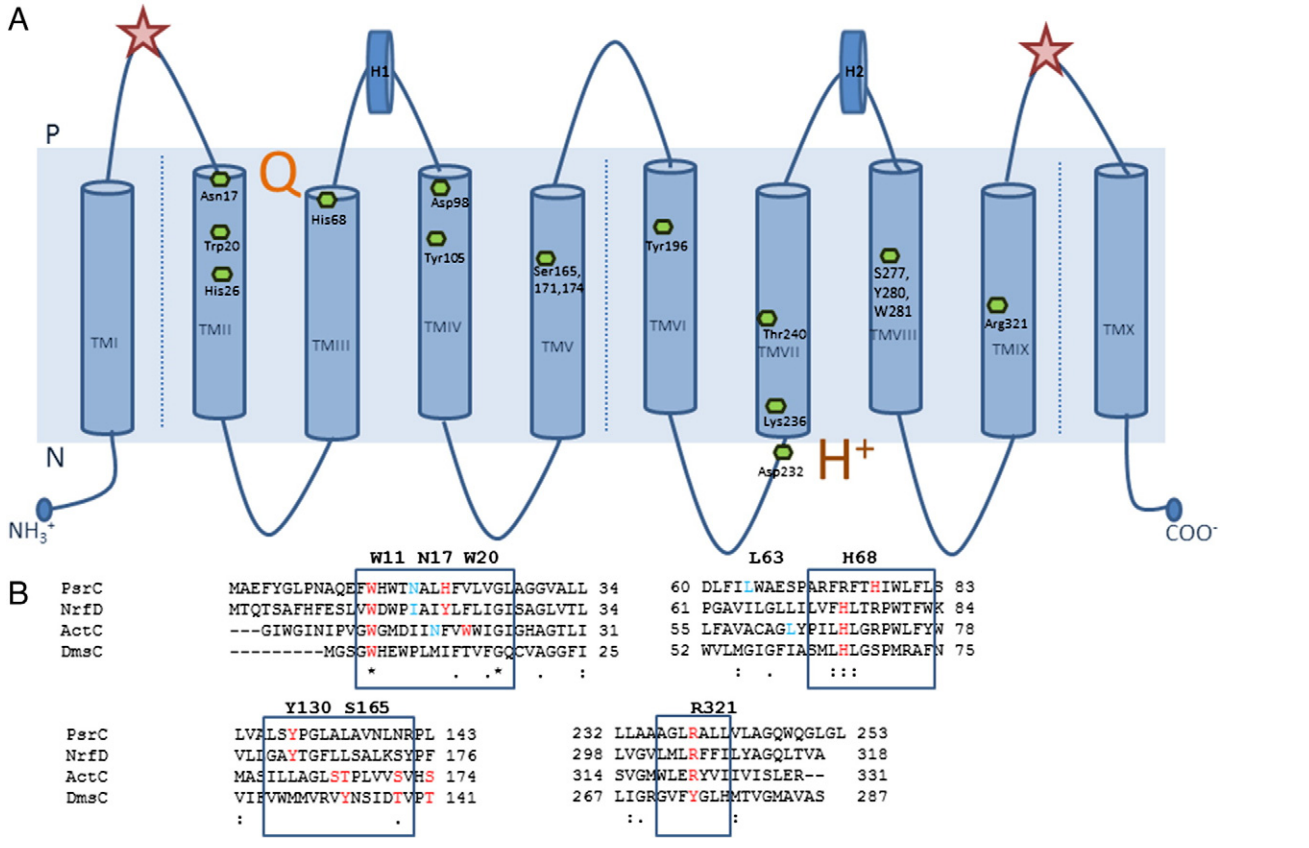

Fig. 3. ActC predicted topology and alignments. A. Predicted topology of ActC. Stars indicate start and end of NrfD domain. Dashed lines indicate predicted regions for four helix bundles. Green hexagons denote approximate location of conserved or biologically relevant amino acid residues. Orange Q and H^+ show possible location of quinone binding site and site of proton uptake respectively. H1 and H2 represent putative periplasmic horizontal helices. B. Alignment of similar integral membrane subunits from the CISM family. Red and blue letters denote conserved or interesting residues and alternate for visual clarity. PsrC is the integral membrane subunit from polysulfide reductase in *T. thermophilus*. NrfD is the integral membrane subunit from nitrite reductase in *E. coli*. ActC is the integral membrane subunit from Alternative Complex III in *C. aurantiacus*. DmsC is the integral membrane subunit from DMSO reductase in *E. coli*.

data [35]. The answer has not as yet been resolved in DmsABC or ACIII and is not likely to be resolved until more structural data is obtained.

3.3. ActC & ActF

ActC and ActF represent the major integral membrane subunits of ACIII. They are highly similar to each other, containing ten transmembrane helices (Supplemental Table 1). ActF is slightly smaller than ActC, with masses of 46 kDa and 55 kDa respectively, and are likely to have resulted from a gene duplication event [8]. While most ACIII's have both ActC and ActF, some species only have ActC (Fig. 1). The middle eight helices of both ActC and ActF have high homology of over 40% to the NrfD protein family (stars, Fig. 3A, Supplemental Table 1). The NrfD family consists of integral membrane proteins that house quinone binding sites [29]. In the NrfD proteins with known structure, these eight helices are arranged in two four-helix bundles [30]. The N-terminal bundle hosts the quinone binding site and the C-terminal bundle is involved in proton translocation and uptake from the cytoplasm.

Because ACIII is an enzyme with menaquinone:auracyanin oxidoreductase activity, the location and amino acid arrangement in the quinone site is of great importance. Previous fluorescence quenching titration work with known quinol oxidation site inhibitor 4-hydroxy-2-heptylquinoline-N-oxide on ACIII has only revealed one quinol oxidation site [18]. Although the possibility of more quinone sites cannot be excluded, any additional quinone sites are more likely to have the role of Q_i sites of the cytochrome *bc* complexes, which are not identified by HQNO assays. To investigate the one identified quinol oxidation site, topology prediction and homology modeling were also carried out for ActC and ActF onto PsrC and PsrG respectively, keeping the model of ActBCF consistent with cross-linking data. Both topology and homology show conservation of hydrophobic amino acids and their positions that create the quinone pocket (green hexagons Fig. 3A, colored residues Fig. 3B). The view of the quinone site highlights the similarity of the hydrophobic pocket, but also reveals the differences that result from binding different quinones. *C. aurantiacus* ACIII uses MK-11, not MK-7 as shown in PSR, so differences in side chain position, especially the primary ligand, are expected to accommodate the longer tail of the menaquinone (Fig. 2C). The ligand to the menaquinone by an H-bond in PSR is a tyrosine on helix five (dashed line, Fig. 2C). Although the ligand tyrosine, Tyr130, is conserved in many NrfD proteins, a tyrosine is not predicted in that location for ACIII so the primary quinone ligand has not been identified at this point (Fig. 3B). Suitable replacements include three serines, Ser165, 171, 174, or Tyr105 on the previous helix, which are all in the pocket and are capable of H-bonding (Fig. 3A & B). Additional conserved H-bonding residues are an asparagine and histidine found at the top of helix one. In ACIII, Asn17 is in the same location at the start of helix II, TMII (green hexagons, Fig. 3A). A histidine, His26, is found later in TMII but a tryptophan, Trp20, is better positioned to be a hydrogen bonding site. Other conserved residues on the N-terminal helix bundle of ACIII include His68 and Asp98, which may contribute to the quinone oxidation cycle [30,37]. Along with PsrB, the two horizontal periplasmic helices put the cap on the quinone pocket and facilitate electron transfer to the iron–sulfur clusters. These features are also seen in the ActB–ActC interface (Figs. 2C, H1 & H2, 3A). Based on the similarity and conservation of residues, the quinol oxidation site of ACIII should resemble that of PSR.

The putative proton-pumping pathway of PSR has many of the same residues or types of residues predicted in similar positions for ACIII within the NrfD domain of ActC [30]. These include: Asp232 for proton uptake from the cytoplasm, other charged residues such as Lys236 and the highly conserved Arg321, and polar residues with alcohol functional groups like Thr240, Tyr196, Ser277, Tyr280 or Trp281 (Fig. 3A & B). The proton channel passes from uptake in the cytoplasm in the C-terminal bundle through the residues listed above, to water molecules that may assist between helix bundles and finally near the Q-site and into the periplasm [30]. Important residues for the primary functions of ACIII, quinone oxidation and proton translocation, are conserved as with other members of the CISM and NrfD families.

The mechanistic implications from the topology and homology model are limited by the facts that ACIII is a monomeric complex with one Fe–S containing subunit and that the model only includes truncated versions of 4 of the 7 subunits of ACIII [15]. Refojo et al. proposed that ACIII is a new architecture that uses modules from other known enzymes [17]. Our modeling of ActABCF connects two of these modules: integral membrane and electron transfer. So, we suggest that the fundamental mechanistic elements of these modules would be conserved along with their structural heritage. The interaction of ActC and ActF to provide a conformationally linked mechanical proton pumping, the interaction at the one identified quinone site with its iron–sulfur subunit, and the flow of electrons in the iron–sulfur clusters should be preserved in the ActABCF model from PsrABCG.

Adding the complexity of the integral membrane subunits is the assembly of respiratory ACIII from *C. aurantiacus*. The gene organization of the respiratory ACIII in *C. aurantiacus* is interesting as it lacks both ActC and F (Fig. 1). Purification of respiratory ACIII revealed that both respiratory and photosynthetic complexes share the photosynthetic ActC and F proteins [8]. This is surprising as the putative operons for both complexes are encoded in entirely different regions of the genome, and the photosynthetic operon shows no obvious way of transcribing ActC or F independently of the entire putative operon. ActC is only two nucleotides from the stop codon in ActB and ActF is 18 nucleotides from the stop codon in Act E. This indicates a complex interplay at the post-transcriptional level to regulate the expression of the photosynthetic and respiratory complexes. Both ActC and F in the photosynthetic operon have ribosome binding sites nine base pairs upstream of their start codons, allowing for independent translation of Act C and F. How respiratory ACIII is regulated and assembled should be an interesting discovery.

3.4. ActD and ActG

ActD and ActG are the least characterized subunits of ACIII. ActD at 20 kDa, is predicted to contain one transmembrane helix and was found to be associated with subunit ActB by a long range crosslinker and ActF by a shorter crosslinking agent [15]. ActD is fused to the pentaheme subunit ActE in genomes belonging to the Planctomycetes phylum (data not shown). ActG is a small, 12 kDa, membrane-associated subunit with unknown function [9]. As demonstrated in *C. aurantiacus*, it can be selectively removed from the complex by chaotropic agents (X. Gao, E. Majumder and R. E. Blankenship, unpublished data). ActG is not found in all ACIII operons. For instance, even though *C. aurantiacus* and *Roseiflexus castenholzii* are closely related photosynthetic bacteria, *R. castenholzii* does not appear to have ActG, as determined from both biochemical and genetic data (Fig. 1). The contribution of these two subunits will become clearer when more is understood about the structure and mechanism of the protein.

3.5. ActE

ActE is a 23 kDa monoheme soluble periplasmic subunit [8]. Despite the abundance of monoheme cytochrome proteins now known, ActE does not have strong similarity to any of them as determined by protein BLAST [39]. With the highest determined redox potential, it is putatively the final member of the electron transfer system in ACIII, accepting electrons from ActA and donating electrons to the soluble electron acceptor and carrier auracyanin or soluble cytochromes. ActE would extend the heme network nanowire that sends electrons over a longer distance efficiently and compensates for apparent mismatch in reduction potentials between donor and acceptor [26]. Recent work has shown ActE to be present in two copies

in *C. aurantiacus* despite a singular copy of *actE* in the operon. For *C. aurantiacus*, the reduction potential of the monoheme cytochrome is +391 mV in the intact complex and +385 mV in the recombinant system, showing agreement between the two systems. ActE has also been shown to be essential for menaquinone:electron acceptor enzyme activity by selectively denaturing the ACIII and measuring the complex activity (X. Gao, E. Majumder and R. E. Blankenship, unpublished data). The two copies of ActE could explain the difference in heme-bound iron content between *R. marinus* and *C. aurantiacus*. *R. marinus* sequence-based analysis places six irons bound in heme, whereas biochemical work in *C. aurantiacus* indicates seven heme-bound irons in the complex [15,17]. The exact role of ActE in ACIII electron transfer remains to be determined as well as its ability to interact with soluble electron carriers, but it is clear that this subunit is critical for enzyme activity.

4. Putative electron transfer mechanism for ACIII

How all of the subunits fit together in ACIII and exactly what function the enzyme is performing in the cell remain unclear. However, the structural clues from its relation to the CISM family and a lack of other proteins in the genome that could replace its activity allow us to make some predictions as to a potential mechanism. From biochemical data like cross-linking and subunit identification, certain subunits are known to be in close proximity or interacting with others [15]. Based on known heme reduction potentials and the preliminary data on Fe–S clusters, we can predict a flow of electrons through the complex [15,27]. It is also believed that this complex pumps protons across the membrane from the lack of a known proton pump in genomes that have ACIII but no cytochrome bc_1 complex. However, experiments to demonstrate this function have yet to be attempted.

Two general electron transfer pathways have been proposed for ACIII: linear and bifurcated [27]. Linear electron flow begins in the quinone site, passing to the iron–sulfur clusters of ActB, then onto the five hemes of ActA, then both hemes in the two copies of ActE and finally onto auracyanin. This pathway is the simplest and limits ACIII to only performing menaquinone:auracyanin oxidoreductase activity. Linear electron flow is the only pathway we have biochemical evidence for at this point. Bifurcated electron transfer would be more like what happens in the cytochrome *bc* complexes, but currently there is no evidence for a Q_i site. Bifurcation in ACIII would have one electron from the quinol oxidation site flow down the iron–sulfur clusters to an unknown acceptor. With the debated orientation of ActB, this could be either a perisplamic or cytoplasmic electron acceptor, neither has been screened for. The second electron would flow down the heme network and to auracyanin completing the known activity of the complex. The exact mechanism in ACIII remains unclear, but it is clear that ACIII should be contributing to cyclic electron transfer and to the establishment of the electrochemical gradient.

5. Electron transport chains involving ACIII

Biochemical and genomic evidence suggests that ACIII can function in photosynthetic and aerobic electron transport chains. Examples of ACIII operons containing a traditional cytochrome caa_3-type and cbb_3-type oxidases are known. The fact that ACIII has become associated with different cytochrome *c* oxidases implies a strong relationship between ACIII and aerobic electron transfer. Additionally, most aerobic ACIII containing organisms lack a cytochrome bc_1 complex [8].

In the Chloroflexi phylum, most members encode an ACIII, although there are several exceptions. The *Dehalococcoides* class and *Herpetosiphon aurantiacus* lack ACIII. *Oscillochloris trichoides* encodes two ACIII copies and a cytochrome bc_1 complex. *C. aurantiacus* also encodes two copies of ACIII. One operon includes a caa_3-type oxidase and is expressed under aerobic growth. The other operon is expressed under photosynthetic growth (Fig. 1). The existence of two copies in *O. trichoides* and *C. aurantiacus* probably functions to separate the aerobic and photosynthetic electron transport chains (Fig. 4). ACIII participates in electron transfer both in photosynthetic and respiratory electron transport chains. In *C. aurantiacus*, light is harvested in the chlorosome and the energy passed into the reaction center [52]. The reaction center reduces quinone to quinol which passes through the membrane to ACIII. ACIII oxidizes quinol to quinone, transporting the protons across the membrane and donating the electrons to the small blue copper protein, auracyanin. Auracyanin acts as the soluble electron transporter and brings the electrons back to the reaction center (Fig. 4A). The respiratory chain has different members but ACIII still serves as the quinol oxidizer and donates electrons to auracyanin (Fig. 4B). Auracyanin will be discussed in the next section.

6. Auracyanins

In order for ACIII to pass electrons to an oxidized reaction center or a terminal oxidase, it is expected to require a periplasmic electron transfer. The blue copper proteins, auracyanins, are hypothesized to fulfill this role in the Chloroflexi bacteria. *C. aurantiacus* encodes four auracyanin genes, labeled A–D [40]. Auracyanins A and B have been purified from *C. aurantiacus* [7]. Initial expression studies of auracyanins A and B suggested that auracyanin A was expressed under photosynthetic growth and auracyanin B was constitutively expressed [41]. However, recent mass spectrometry data comparing photosynthetic and aerobic growth showed the opposite trend with auracyanin A being expressed under aerobic growth and auracyanin B being expressed under photosynthetic growth [42]. Unpublished western blot data from the authors confirmed the mass spectrometry result (J. King, E. Majumder, and R. E. Blankenship). Auracyanins C and D have never been detected biochemically, but are known from genomic evidence [40]. All four proteins have been expressed in *E. coli*. The *E. coli* expressed auracyanins A and B lack the glycosylation and lipidation normally present in those derived from *C. aurantiacus*. However, the redox potential and spectra are unchanged [41]. Recombinant auracyanins C and D are currently being characterized. An additional auracyanin has been characterized from the related *R. castenholzii*; this auracyanin will be referred to as auracyanin RC. Studies on the native and recombinant forms of auracyanins have led to a good understanding of their structures and some predictions of their functions.

6.1. Structure of auracyanins

Auracyanins A and B both have solved crystal structures (Fig. 5) [41,45]. Like other Type 1 blue copper proteins, the auracyanins have eight beta strands arranged in two sheets. The arrangement of the beta strands forms a Greek-key fold (Fig. 5A). The copper ion is sandwiched between the two sheets and is coordinated by a cysteine thiolate, two histidine imidazoles, and a methionine thioether. The cysteine, one of the histidines, and the methionine can all be found in the loop between beta strand 7 and 8. The axial methionine ligand is weakly bonded, resulting in a geometry that can be described as a distorted trigonal-pyramidal [41]. The ligand geometry is essentially identical between auracyanins A and B (Fig. 5B). This is surprising as UV–vis, circular dichroism, resonance Raman, and electron paramagnetic resonance predicted highly different copper sites [7]. However, the ligand distances and geometries calculated from the crystals were confirmed by XAS on solutions of auracyanins A and B [41].

Blue copper proteins interact with their redox partners near the copper site [43,44]. This is unsurprising as electron transfer efficiency falls off exponentially with distance. The regions labeled “north” and “east” in Fig. 5A are primarily responsible for the docking in other blue copper proteins. Electron transfer is thought to proceed from the copper site through the top of the “northern” face. The distance from the northern face of the auracyanins to the surface is 6 Å.

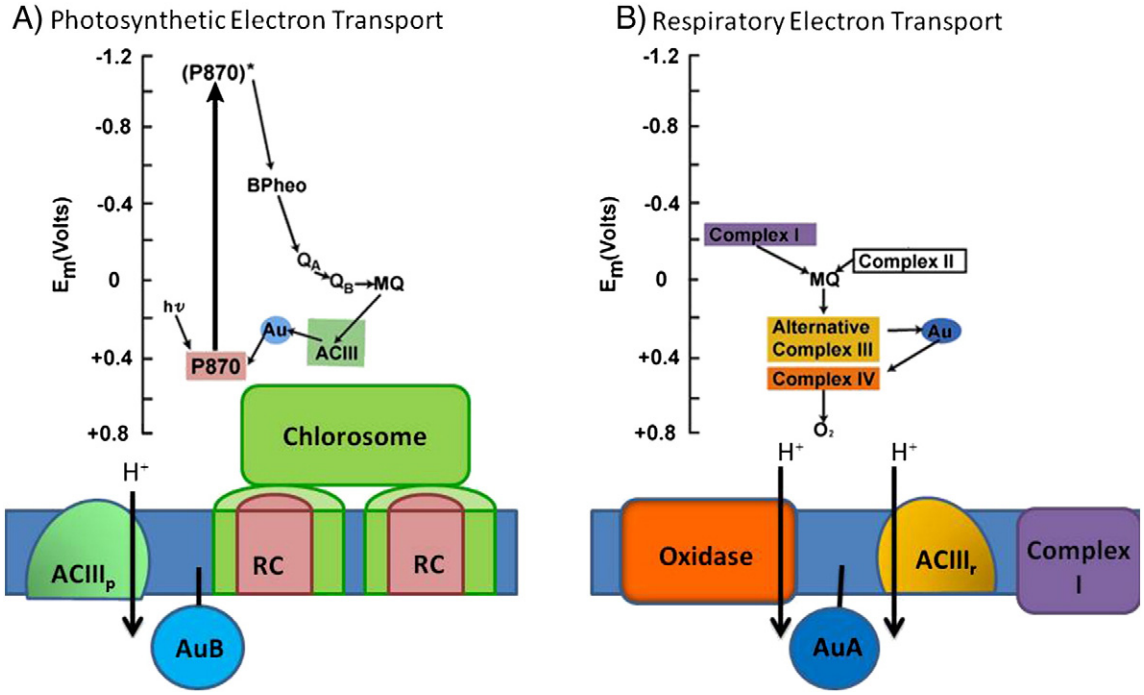

Fig. 4. Photosynthetic and respiratory electron transport chains in *C. aurantiacus*. A. Photosynthetic electron transport chain. B. Respiratory electron transport chain Z-scheme shows energy level throughout cyclic electron transport. RC is the reaction center which holds the P870 pigment, bacteriopheophytin pigment, QA and QB sites. MQ is menaquinone. Au is auracyanin. TCA is the tricarboxylic acid cycle. Oxidase is cytochrome *c* oxidase or Complex IV.

Auracyanins A and B have hydrophobic patches on their "northern" face [41]. However, auracyanin B has many polar residues not present in auracyanin A in this region [45]. Auracyanin B also has evidence of glycosolation [7]. The poorly conserved "variable region" between beta strands 4 and 5 of blue copper proteins is fairly similar between auracyanins A and B. This region is thought to be important for redox interactions in other blue copper proteins [45]. The surface similarities with minor differences suggest that auracyanins A and B might have similar, but distinct redox partners.

Sequence alignment leads to several interesting predictions about auracyanins C and D. First, the first coordinating histidine is followed by a glutamic acid in auracyanin C and a serine in auracyanin D. This residue is normally conserved as an asparagine in all other blue copper proteins. Changing this asparagine to a serine led to an increase of +130 mV in the redox potential of the blue copper protein azurin [46]. Second, sequence alignment suggests that auracyanin D has a glutamine axial ligand. Glutamine is occasionally seen as an axial ligand in blue copper proteins. Replacing the typical methionine with glutamine in azurin resulted in 263 mV decrease in potential [46,47]. Finally, it is worth noting that the variable region is poorly conserved between auracyanins C and D in *C. aurantiacus*, yet fairly conserved in other auracyanins. This suggests that auracyanins C and D may have novel functions.

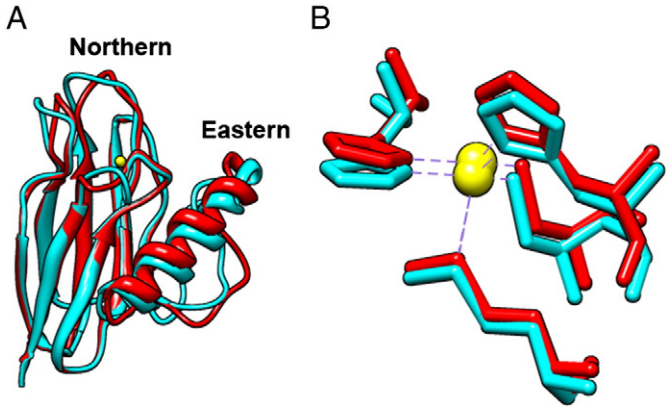

Fig. 5. Structure of auracyanin. A. Overall structural comparison of auracyanins A and B. B. Comparison of ligand geometry of auracyanins A and B. In B, the overlay of auracyanins A and B has been displaced slightly for clarity. Auracyanin A is shown in red and auracyanin B is shown in cyan. Copper atom is shown in gold.

6.2. Localization of auracyanins

Auracyanins A and B are both membrane anchored, and hypothesized to be periplasmic based on putative signal peptides. Auracyanin A appears to be a lipoprotein. Mass spectrometry suggests that auracyanin A contains an acetyl-N-cysteine-S-glycerol modification at its amino terminus. This group is attached to the protein at a cysteine residue following the signal peptide [48]. This cysteine residue is conserved in all auracyanins except for auracyanin B and the auracyanin B homologue from *O. trichoides* DG6. The cysteine is flanked by conserved alanine and glycine. The +2 rule for bacterial lipoproteins predicts that auracyanin A with a glycine in the +2 position would be mostly chaperoned to the outer membrane [49]. However, recent arguments have suggested that Chloroflexi bacteria are monoderm (i.e. lacking an outer membrane) [50]. Additionally, the LolAB chaperones that function in gram-negative bacteria as the chaperones responsible for moving lipoproteins to the outer membrane appear to be lacking in the Chloroflexi genomes. As a result, we place auracyanin attached to the cytoplasmic membrane but facing into the periplasmic or equivalent space. However, it is unresolved if Chloroflexi are truly monoderm, and Chloroflexi bacteria could use different lipoprotein processing machinery as they are evolutionarily very distant from bacteria whose lipoprotein pathway has been characterized. Thus, it is possible that auracyanin A is transported to an outer membrane via an unknown mechanism.

Auracyanin B and the auracyanin B-like protein from *O. trichoides* DG6 are unique among the auracyanins in that they lack the conserved lipid signal. Instead, both proteins have an extended N-terminal region

containing a putative transmembrane domain [48]. Interestingly, *C. aurantiacus* and *O. trichoides* are examples of photosynthetic Chloroflexi bacteria that use a chlorosome antenna for light harvesting [51]. This antenna is found attached to the cytoplasmic side of the inner cell membrane. It is assumed that the reaction center and photosynthetic electron transport chains are also restricted to certain domains [52]. Expression data suggests that auracyanin B is expressed during photosynthetic growth [42]. Thus, the replacement of the lipid signal with a transmembrane domain may limit auracyanin B to regions of membrane associated with photosynthetic electron transport.

6.3. Evidence supporting auracyanins as a mobile electron carrier

There exists a debate as to whether the auracyanins in fact perform the periplasmic respiratory and photosynthetic electron transfers. Initially, auracyanin seemed like the ideal candidate as both auracyanin A and B could reduce purified reaction centers in *C. aurantiacus* [7]. This was further supported by the ability of auracyanin A to oxidize purified ACIII from *C. aurantiacus* [9]. However, spectroscopic studies on membrane from the related FAP *R. castenholzii* showed no photoreduction in the presence of auracyanin RC. The authors of this paper suggest that the protocol used, which was optimized for purple bacteria, may not work in *R. castenholzii*. Alternatively, *R. castenholzii* may use a different electron carrier [53].

A second argument against auracyanin as the mobile carrier is the redox mismatch between the auracyanins and ACIII. Auracyanin A ($E_{m,7} = 205 \pm 7$ mV) and B ($E_{m,7} = 215 \pm 7$ mV) have redox potentials well below their proposed ACIII redox partner ActE ($E_{m,7} = +391$ mV) [15,54]. Such an uphill reaction is thermodynamically unfavorable. Despite this difference, reduced ACIII is able to reduce oxidized auracyanin A in solution. It is possible that ActE is not the auracyanin redox partner, as proposed. Alternatively, it is well documented that the blue copper protein amicyanin's potential changes upon binding to its redox partners, allowing an otherwise uphill reaction to occur [55]. Another possibility is that an uphill reaction between ActE and auracyanin occurs, but the driving force from menaquinol to auracyanin is enough to overcome this. Such a process is known to happen in the tetraheme subunit of the reaction center of purple bacteria [56].

Compared with other photosynthetic systems, *C. aurantiacus* could use a cytochrome *c* or blue copper protein to reduce the reaction center [57]. The auracyanins are a favorable option due to their high abundance in the cell. In purple bacteria, electrons are carried from the cytochrome bc_1 complex to the reaction center by the soluble proteins cytochrome c_2 or HiPIP [57]. The *C. aurantiacus* J-10-fl genome lacks any genes encoding a HiPIP using the PFAM definition (PFAM01355). However, the genome has genes for two possible cytochrome *c* proteins (Caur_0845 and Caur_0980). Caur_0980 is on an operon with bilirubin oxidase, and likely functions in the heme degradation pathway. Caur_0845 appears to be monocistronic, and could function in electron transport. However, neither cytochrome *c*'s have been detected by heme staining [5] or mass spectrometry [42]. It is possible that one of the cytochrome *c* proteins functions in electron transport, but is below traditional detection limits. It is also possible that *C. aurantiacus* could use a novel mechanism to carry electrons from ACIII to the reaction center that does not involve a blue copper protein, a HiPIP, or a cyt *c*. With these possibilities in mind, auracyanins still seem like the most likely mobile electron carriers. Additional experiments on ACIII's redox pathway and enzyme activity assays should clarify this issue.

7. Concluding thoughts

The electron transport chains in many phototrophic bacteria still remain to be characterized and understood. ACIII and its soluble electron acceptor auracyanin are among the more unusual members of those electron transport chains. Homology to related enzymes has provided significant clues to structure and mechanism, especially when coupled with existing biochemical data. Understanding of auracyanin is developing and revealing new limits for blue copper proteins. A complete understanding of the ACIII–auracyanin system will enhance our knowledge of the photosynthetic mechanisms of bacteria, particularly Chloroflexi.

Acknowledgements

We would like to acknowledge Hao Zhang for his help in interpreting the mass spectrometry results.

Online software used in this review: BLAST, Chimera, ClustalW, GenTHREADER, Modeller, Plotcon by EMBOSS, PSIPRED, SOSUI, SMART, and TopPred.

Molecular graphics and analyses were performed with the UCSF Chimera package. Chimera is developed by the Resource for Biocomputing, Visualization, and Informatics at the University of California, San Francisco, with support from the National Institutes of Health (National Center for Research Resources grant 2P41RR001081, National Institute of General Medical Sciences grant 9P41GM103311).

This study utilized the high-performance computational capabilities of the Helix Systems at the National Institutes of Health, Bethesda, MD (http://helix.nih.gov).

This work was supported by grant #MCB-0646621 to R.E.B. from the Molecular Biochemistry Program of NSF, the Olin Fellowship for Women to ELWM, and Monsanto Graduate Fellowship to JDK.

Appendix A. Supplementary data

Supplementary data to this article can be found online at http://dx.doi.org/10.1016/j.bbabio.2013.01.008.

References

[1] R.E. Blankenship, Molecular Mechanisms of Photosynthesis, Blackwell Science, Oxford, 2002.
[2] B.K. Pierson, R.W. Castenholz, A phototrophic gliding filamentous bacterium of hot springs, *Chloroflexus aurantiacus*; gen. and sp. nov, Arch. Microbiol. 100 (1974) 5–24.
[3] G. Strauss, G. Fuchs, Enzymes of a novel autotrophic CO_2 fixation pathway in the phototrophic bacterium *Chloroflexus aurantiacus*, the 3-hydroxypropionate cycle, Eur. J. Biochem. 215 (1993) 633–643.
[4] R.E. Blankenship, R. Feick, B.D. Bruce, C. Kirmaier, D. Holten, R.C. Fuller, Primary photochemistry in the facultative green photosynthetic bacterium *Chloroflexus aurantiacus*, J. Cell. Biochem. 22 (1983) 251–261.
[5] B. Pierson, Cytochromes in *Chloroflexus aurantiacus* grown with and without oxygen, Arch. Microbiol. 143 (1985) 260–265.
[6] J. Trost, J. Mcmanus, J. Freeman, B. Ramakrishna, R. Blankenship, Auracyanin, a blue copper protein from the green photosynthetic bacterium *Chloroflexus aurantiacus*, Biochemistry 27 (1988) 7858–7863.
[7] J.D. McManus, D.C. Brune, J. Han, J. Sanders-Loehr, T.E. Meyer, M.A. Cusanovich, G. Tollin, R.E. Blankenship, Isolation, characterization, and amino acid sequences of auracyanins, blue copper proteins from the green photosynthetic bacterium *Chloroflexus aurantiacus*, J. Biol. Chem. 267 (1992) 6531–6540.
[8] M. Yanyushin, M. del Rosario, D. Brune, R. Blankenship, New class of bacterial membrane oxidoreductases, Biochemistry 44 (2005) 10037–10045.
[9] X. Gao, Y. Xin, R. Blankenship, Enzymatic activity of the alternative complex III as a menaquinol:auracyanin oxidoreductase in the electron transfer chain of *Chloroflexus aurantiacus*, FEBS Lett. 583 (2009) 3275–3279.
[10] M.M. Pereira, A.M. Antunes, O.C. Nunes, M.S. Dacosta, M. Teixeira, A membrane-bound HiPIP type center in the thermohalophile—*Rhodothermus marinus*, FEBS Lett. 352 (1994) 327–330.
[11] R.M. Wynn, T.E. Redlinger, J.M. Foster, R.E. Blankenship, R.C. Fuller, R.W. Shaw, D.B. Knaff, Electron-transport chains of phototrophically and chemotrophically grown *Chloroflexus aurantiacus*, Biochim. Biophys. Acta (BBA) — Bioenerg. 891 (1987) 216–226.
[12] M.M. Pereira, J.N. Carita, M. Teixeira, Membrane-bound electron transfer chain of the thermohalophilic bacterium *Rhodothermus marinus*: a novel multihemic cytochrome *bc*, a new complex III, Biochem. (Easton) 38 (1999) 1268–1275.
[13] M.F. Yanyushin, Fractionation of cytochromes of phototrophically grown *Chloroflexus aurantiacus*. Is there a cytochrome *bc* complex among them? FEBS Lett. 512 (2002) 125–128.
[14] M.M. Pereira, J.N. Carita, M. Teixeira, Membrane-bound electron transfer chain of the thermohalophilic bacterium *Rhodothermus marinus*: characterization of the iron–sulfur centers from the dehydrogenases and investigation of the high-potential

iron–sulfur protein function by in vitro reconstitut, Biochem. (Easton) 38 (1999) 1276–1283.
[15] X. Gao, Y. Xin, P.D. Bell, J. Wen, R.E. Blankenship, Structural analysis of alternative complex III in the photosynthetic electron transfer chain of *Chloroflexus aurantiacus*, Biochemistry 49 (2010) 6670–6679.
[16] M.M. Pereira, P.N. Refojo, G.O. Hreggvidsson, S. Hjorlelfsdottir, M. Teixeira, The alternative complex III from *Rhodothermus marinus* — a prototype of a new family of quinol:electron acceptor oxidoreductases, FEBS Lett. 581 (2007) 4831–4835.
[17] P.N. Refojo, F.L. Sousa, M. Teixeira, M.M. Pereira, The alternative complex III: a different architecture using known building modules, Quinone Bind. Catal. 1797 (2010) 1869–1876.
[18] P.N. Refojo, M. Teixeira, M.M. Pereira, The alternative complex III of *Rhodothermus marinus* and its structural and functional association with caa(3) oxygen reductase, Biochim. Biophys. Acta Bioenerg. 1797 (2010) 1477–1482.
[19] T. Hirokawa, S. Boon-Chieng, S. Mitaku, SOSUI: classification and secondary structure prediction system for membrane proteins, Bioinformatics 14 (1998) 378–379.
[20] J. Schultz, F. Milpetz, P. Bork, C.P. Ponting, SMART, a simple modular architecture research tool: identification of signaling domains, Proc. Natl. Acad. Sci. 95 (1998) 5857–5864.
[21] T.A. Clarke, V. Dennison, H.E. Seward, B. Burlat, J.A. Cole, A.M. Hemmings, D.J. Richardson, Purification and spectropotentiometric characterization of *Escherichia coli* NrfB, a decaheme homodimer that transfers electrons to the decaheme periplasmic nitrite reductase complex, J. Biol. Chem. 279 (2004) 41333–41339.
[22] T.A. Clarke, J.A. Cole, D.J. Richardson, A.M. Hemmings, The Crystal Structure of the Pentahaem *c*-type Cytochrome NrfB and Characterization of its Solution-state Interaction with the Pentahaem Nitrite Reductase NrfA, 2007.
[23] M.A. Larkin, G. Blackshields, N.P. Brown, R. Chenna, P.A. McGettigan, H. McWilliam, F. Valentin, I.M. Wallace, A. Wilm, R. Lopez, J.D. Thompson, T.J. Gibson, D.G. Higgins, Clustal W and Clustal X version 2.0, Bioinformatics 23 (2007) 2947–2948.
[24] N. Eswar, B. Webb, M.A. Marti-Renom, M.S. Madhusudhan, D. Eramian, M.-Y. Shen, U. Pieper, A. Sali, Comparative protein structure modeling using Modeller, Current Protocols in Bioinformatics, John Wiley & Sons, Inc., 2002
[25] E.F. Pettersen, T.D. Goddard, C.C. Huang, G.S. Couch, D.M. Greenblatt, E.C. Meng, T.E. Ferrin, UCSF Chimera—a visualization system for exploratory research and analysis, J. Comput. Chem. 25 (2004) 1605–1612.
[26] P.R. Pokkuluri, Y.Y. Londer, N.E.C. Duke, M. Pessanha, X. Yang, V. Orshonsky, L. Orshonsky, J. Erickson, Y. Zagyanskiy, C.A. Salgueiro, M. Schiffer, Structure of a novel dodecaheme cytochrome c from *Geobacter sulfurreducens* reveals an extended 12 nm protein with interacting hemes, J. Struct. Biol. 174 (2011) 223–233.
[27] P.N. Refojo, M. Teixeira, M.M. Pereira, The Alternative complex III: Properties and possible mechanisms for electron transfer and energy conservation, Biochim. Biophys. Acta Bioenerg. 1817 (2012) 1852–1859.
[28] L.A. Sazanov, P. Hinchliffe, Structure of the hydrophilic domain of respiratory complex I from *Thermus thermophilus*, Science (New York, N.Y.) 311 (2006) 1430–1436.
[29] R.A. Rothery, G.J. Workun, J.H. Weiner, The prokaryotic complex iron–sulfur molybdoenzyme family, Biochim. Biophys. Acta 1778 (2008) 1897–1929.
[30] M. Jormakka, K. Yokoyama, T. Yano, M. Tamakoshi, S. Akimoto, T. Shimamura, P. Curmi, S. Iwata, Molecular mechanism of energy conservation in polysulfide respiration, Nat. Struct. Mol. Biol. 15 (2008) 730–737.
[31] B.C. Berks, F. Sargent, T. Palmer, The Tat protein export pathway, Mol. Microbiol. 35 (2000) 260–274.
[32] I. Bertini, H.B. Gray, E.I. Steifel, J.S. Valentine, Biological Inorganic Chemistry: Structure and Reactivity, University Science Books, Sausalito, 2007.
[33] D.T. Jones, Protein secondary structure prediction based on position-specific scoring matrices, J. Mol. Biol. 292 (1999) 195–202.
[34] G. von Heijne, Membrane protein structure prediction: hydrophobicity analysis and the positive-inside rule, J. Mol. Biol. 225 (1992) 487–494.
[35] R.A. Rothery, N. Kalra, R.J. Turner, J.H. Weiner, Sequence similarity as a predictor of the transmembrane topology of membrane-intrinsic subunits of bacterial respiratory chain enzymes, J. Mol. Microbiol. Biotechnol. 4 (2002) 133–150.
[36] P.T. Bilous, J.H. Weiner, Proton translocation coupled to dimethyl sulfoxide reduction in anaerobically grown *Escherichia coli* HB101, J. Bacteriol. 163 (1985) 369–375.
[37] P. Geijer, J.H. Weiner, Glutamate 87 is important for menaquinol binding in DmsC of the DMSO reductase (DmsABC) from *Escherichia coli*, Biochim. Biophys. Acta Rev. Biomembr. 1660 (2004) 66–74.
[38] F. Schneider, J. Löwe, R. Huber, H. Schindelin, C. Kisker, J. Knäblein, Crystal structure of dimethyl sulfoxide reductase from *Rhodobacter capsulatus* at 1.88 A resolution, J. Mol. Biol. 263 (1996) 53–69.
[39] S.F. Altschul, W. Gish, W. Miller, E.W. Myers, D.J. Lipman, Basic local alignment search tool, J. Mol. Biol. 215 (1990) 403–410.
[40] K.-H. Tang, K. Barry, O. Chertkov, E. Dalin, C. Han, L. Hauser, B. Honchak, L. Karbach, M. Land, A. Lapidus, F. Larimer, N. Mikhailova, S. Pitluck, B. Pierson, R. Blankenship, Complete genome sequence of the filamentous anoxygenic phototrophic bacterium *Chloroflexus aurantiacus*, BMC Genomics 12 (2011) 334.
[41] M. Lee, M. del Rosario, H. Harris, R. Blankenship, J. Guss, H. Freeman, The crystal structure of auracyanin A at 1.85 Å resolution: the structures and functions of auracyanins A and B, two almost identical "blue" copper proteins, in the photosynthetic bacterium *Chloroflexus aurantiacus*, J. Biol. Inorg. Chem. 14 (2009) 329–345.
[42] L. Cao, D.A. Bryant, A.A. Schepmoes, K. Vogl, R. Smith, M. Lipton, S. Callister, Comparison of *Chloroflexus aurantiacus* strain J-10-fl proteomes of cells grown chemoheterotrophically and photoheterotrophically, Photosynth. Res. 110 (2012) 153–168.
[43] I. Díaz-Moreno, A. Díaz-Quintana, M.A. De la Rosa, M. Ubbink, Structure of the complex between plastocyanin and cytochrome f from the cyanobacterium *Nostoc* sp. PCC 7119 as determined by paramagnetic NMR, J. Biol. Chem. 280 (2005) 18908–18915.
[44] F. Meschi, F. Wiertz, L. Klauss, C. Cavalieri, A. Blok, B. Ludwig, H.A. Heering, A. Merli, G.L. Rossi, M. Ubbink, Amicyanin transfers electrons from methylamine dehydrogenase to cytochrome *c*-551i via a ping–pong mechanism, not a ternary complex, J. Am. Chem. Soc. 132 (2010) 14537–14545.
[45] C.S. Bond, R.E. Blankenship, H.C. Freeman, J.M. Guss, M.J. Maher, F.M. Selvaraj, M.C.J. Wilce, K.M. Willingham, Crystal structure of auracyanin, a "blue" copper protein from the green thermophilic photosynthetic bacterium *Chloroflexus aurantiacus*, J. Mol. Biol. 306 (2001) 47–67.
[46] N.M. Marshall, D.K. Garner, T.D. Wilson, Y.-G. Gao, H. Robinson, M.J. Nilges, Y. Lu, Rationally tuning the reduction potential of a single cupredoxin beyond the natural range, Nature 462 (2009) 113–116.
[47] A. Romero, C.W.G. Hoitink, H. Nar, R. Huber, A. Messerschmidt, G.W. Canters, X-ray analysis and spectroscopic characterization of M121Q azurin: a copper site model for stellacyanin, J. Mol. Biol. 229 (1993) 1007–1021.
[48] G.V. Driessche, W. Hu, G.V.D. Werken, F. Selvaraj, J.D. McManus, R.E. Blankenship, J.J. Van Beeumen, Auracyanin a from the thermophilic green gliding photosynthetic bacterium *Chloroflexus aurantiacus* represents an unusual class of small blue copper proteins, Protein Sci. 8 (1999) 947–957.
[49] A. Seydel, P. Gounon, A.P. Pugsley, Testing the '+2 rule' for lipoprotein sorting in the *Escherichia coli* cell envelope with a new genetic selection, Mol. Microbiol. 34 (1999) 810–821.
[50] I.C. Sutcliffe, Cell envelope architecture in the Chloroflexi: a shifting frontline in a phylogenetic turf war, Environ. Microbiol. 13 (2011) 279–282.
[51] S. Hanada, B. Pierson, The Family Chloroflexaceae, in: M. Dworkin, S. Falkow, E. Rosenberg, K.H. Schleifer, E. Stackebrandt (Eds.), The Prokaryotes, Springer, New York, 2006, pp. 815–842.
[52] R. Blankenship, K. Matsuura, Antenna complexes from green photosynthetic bacteria, Anoxygenic Photosynth. Bact. (2003) 195–217.
[53] Y. Tsukatani, N. Nakayama, K. Shimada, H. Mino, S. Itoh, K. Matsuura, S. Hanada, K.V.P. Nagashima, Characterization of a blue-copper protein, auracyanin, of the filamentous anoxygenic phototrophic bacterium *Roseiflexus castenholzii*, Arch. Biochem. Biophys. 490 (2009) 57–62.
[54] M. Rooney, M. Honeychurch, F. Selvaraj, R. Blankenship, A. Bond, H. Freeman, A thin-film electrochemical study of the "blue" copper proteins, auracyanin A and auracyanin B, from the photosynthetic bacterium *Chloroflexus aurantiacus* the reduction potential as a function of pH, J. Biol. Inorg. Chem. 8 (2003) 306–317.
[55] Z. Zhu, L.M. Cunane, Z.-w. Chen, R.C.E. Durley, F.S. Mathews, V.L. Davidson, Molecular basis for interprotein complex-dependent effects on the redox properties of amicyanin, Biochemistry 37 (1998) 17128–17136.
[56] I.P. Chen, P. Mathis, J. Koepke, H. Michel, Uphill electron transfer in the tetraheme cytochrome subunit of the *Rhodopseudomonas viridis* photosynthetic reaction center: evidence from site-directed mutagenesis, Biochemistry 39 (2000) 3592–3602.
[57] T. Meyer, M. Cusanovich, Discovery and characterization of electron transfer proteins in the photosynthetic bacteria, Photosynth. Res. 76 (2003) 111–126.